Magnetic fragmentation and fractionalized Goldstone modes in a bilayer quantum spin liquid

Aayush Vijayvargia, ¹ Emilian Marius Nica, ^{1,2} Roderich Moessner, ³ Yuan-Ming Lu, ⁴ and Onur Erten ¹ Department of Physics, Arizona State University, Tempe, Arizona 85287, USA ² Department of Physics and Astronomy, Rice University, 6100 Main St, Houston 77005 Texas, USA ³ Max-Planck-Institut für Physik komplexer Systeme, Nöthnitzer Strasse 38, 01187 Dresden, Germany ⁴ Department of Physics, The Ohio State University, Columbus Ohio 43210, USA



(Received 15 March 2023; accepted 7 June 2023; published 22 June 2023; corrected 22 April 2024)

We study the phase diagram of a bilayer quantum spin liquid model with Kitaev-type interactions on a square lattice. We show that the low energy limit is described by a π -flux Hubbard model with an enhanced SO(4) symmetry. The antiferromagnetic Mott transition of the Hubbard model signals a magnetic fragmentation transition for the spin and orbital degrees of freedom of the bilayer. The fragmented "Néel order" features a nonlocal string order parameter for an in-plane Néel component, in addition to an anisotropic local order parameter. The associated quantum order is characterized by an emergent $\mathbb{Z}_2 \times \mathbb{Z}_2$ gauge field when the Néel vector is along the \hat{z} direction, and a \mathbb{Z}_2 gauge field otherwise. We underpin these results with a perturbative calculation, which is consistent with the field theory analysis. We conclude with a discussion on the low energy collective excitations of these phases and show that the Goldstone boson of the $\mathbb{Z}_2 \times \mathbb{Z}_2$ phase is fractionalized and nonlocal.

DOI: 10.1103/PhysRevResearch.5.L022062

Introduction. Quantum spin liquids (QSLs) are frustrated magnets that do not exhibit long range magnetic order down to zero temperature [1–4]. Quantum fluctuations in these systems give rise to exotic phenomena such as fractionalization and long-range entanglement, which now become the defining properties for QSLs [5–7]. The Kitaev model on the honeycomb lattice [8] is one of the few examples of an exactly solvable model with a QSL ground state (GS). In recent years, remarkable progress in identifying candidate materials with strong Kitaev-type interactions has been achieved in such instances as the iridates [9,10] and α -RuCl₃ [11]. Kitaev interactions may also be strong in other van der Waals (vdW) materials [12]. Bilayers and moiré superlattices of vdW materials are new tunable quantum platforms for realizing a multitude of novel phases with a variety of basic building blocks including graphene [13], semiconductors [14], and superconductors [15].

Motivated by these developments, we study the phase diagram of a bilayer QSL model with Kitaev-type interactions on a square lattice [see Fig. 1(a)]. First introduced in Ref. [16], the exact ground state of the monolayer model is an algebraic QSL featuring two flavors of Majorana fermions that are delocalized on the π -flux square lattice and gapped π -flux (vison) excitations [17]. In the bilayer model Eq. (1), we add an Ising-type interlayer spin interaction, which commutes with the intralayer flux operators and hence allows for controlled calculations. Our main results are summarized as follows: (i)

Published by the American Physical Society under the terms of the Creative Commons Attribution 4.0 International license. Further distribution of this work must maintain attribution to the author(s) and the published article's title, journal citation, and DOI.

Below the vis n gap, we map the low-energy subspace of the bilayer model to a π -flux Hubbard model at half-filling with an emergent SO(4) symmetry. Monte Carlo studies of this model show an antiferromagnetic (AFM) Mott transition at critical $U_c \sim 6t$ [18,19]. (ii) The in-plane components of the AFM order parameter, i.e., $n^{x,y}$ of the Néel vector **n**, correspond to nonlocal order parameters whereas the out-of-plane component (n^z) is a local order parameter in terms of the spin and orbital degrees of freedom (DOF) of the bilayer system. The coexistence of topological order and local order, akin to spin ice models, is observed in our study and is referred to as magnetic fragmentation [20]. (iii) The system features a $\mathbb{Z}_2 \times \mathbb{Z}_2$ gauge field when the Néel vector points along \hat{z} , and a \mathbb{Z}_2 gauge field otherwise. (iv) To complement the results of the Hubbard model, we perturbatively derive an effective Hamiltonian in the limit of large interlayer interactions. We confirm the magnetic fragmentation and topological degeneracy directly in terms of the original DOF, which are consistent with the Majorana fermion representation of the spin model. (v) We show that the Goldstone modes of the fragmented AFM order is fractionalized in the $\mathbb{Z}_2 \times \mathbb{Z}_2$ phase, in comparison to the normal Goldstone modes in the \mathbb{Z}_2 phase.

Microscopic model. One of the key conditions for the exact solution of the Kitaev model is the anticommutation relations of the Pauli matrices, $\{\sigma_i, \sigma_j\} = 2\delta_{ij}$. Since there are only three Pauli matrices, this method can only be applied to lattices with coordination number z=3 such as honeycomb, hyperhoneycomb, and hyperoctagon lattices. However, it is possible to extend Kitaev's method to Γ matrices that obey the Clifford algebra $\{\Gamma_i, \Gamma_j\} = 2\delta_{ij}$ [21,22]. For instance, for a four-dimensional representation of the Clifford algebra, there are five Γ^{α} operators along with ten $\Gamma^{\alpha\beta} = \frac{i}{2}[\Gamma^{\alpha}, \Gamma^{\beta}]$ and an identity matrix, which span the local Hilbert space.

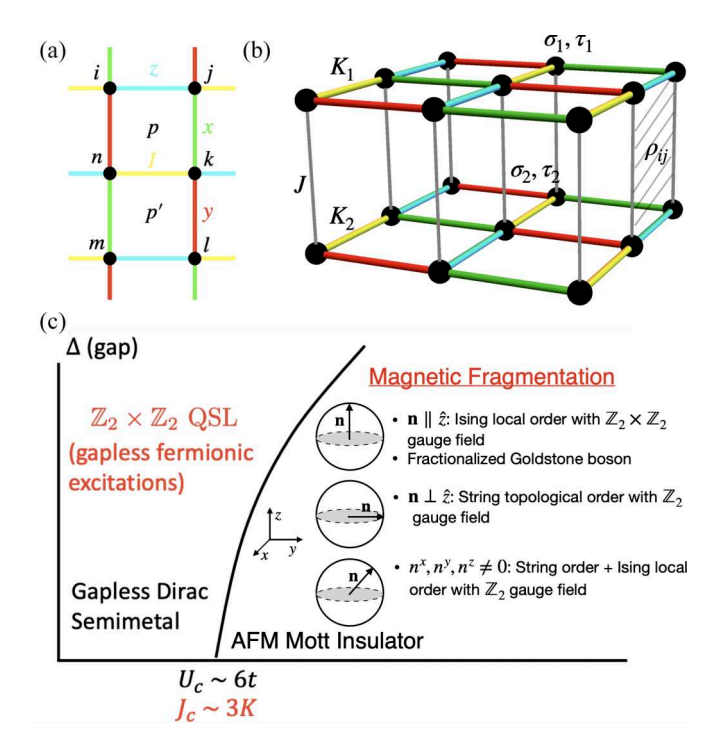


FIG. 1. Schematic of the model and the phase diagram: (a) single layer unit cell. Four different colors depict four types of bonds. There are two inequivalent plaquettes p and p' in a unit cell. (b) Bilayer model with intralayer Kitaev parameters K_{ν} and an interlayer exchange, J. (c) The low-energy description of the model is a π -flux Hubbard model which exhibits a Mott transition at $U/t \sim 6$ (black). In terms of the original degrees of freedom, the Mott transition corresponds to a magnetic fragmentation transition where a local magnetic order coexists with a nonlocal topological order.

Therefore, Kitaev's construction can be extended to lattices with coordination number up to z=5 [21,22]. We adapt this representation and consider the intralayer Hamiltonian [16], $H_K=-\sum_{\langle ij\rangle_{\gamma},\nu}K_{\nu}(\Gamma^{\gamma}_{\nu i}\Gamma^{\gamma}_{\nu j}+\Gamma^{\gamma 5}_{\nu i}\Gamma^{\gamma 5}_{\nu j})$, where $\nu=1,2$ is the layer index and γ is the type of the bond as depicted in Fig. 1. We also introduce an interlayer Ising interaction $H_J=J\sum_i\Gamma^5_{1i}\Gamma^5_{2i}$. The full Hamiltonian can be expressed in terms of spins (σ) and orbital (τ) Pauli matrices using the relation $\Gamma^{\alpha}=-\sigma^y\otimes\tau^{\alpha}$ $(\alpha=x,y,z),\ \Gamma^4=\sigma^x\otimes\mathbb{I}_2$, and $\Gamma^5=-\sigma^z\otimes\mathbb{I}_2$,

$$H = H_K + H_J = -\sum_{\langle ij\rangle_{\gamma},\nu} K_{\nu} \left(\sigma_{\nu i}^x \sigma_{\nu j}^x + \sigma_{\nu i}^y \sigma_{\nu j}^y\right) \left(\tau_{\nu i}^{\gamma} \tau_{\nu j}^{\gamma}\right)$$

$$+ J \sum_{i} \sigma_{1i}^z \sigma_{2i}^z. \tag{1}$$

Here, $\tau^{\gamma} = \tau^{x}$, τ^{y} , τ^{z} , \mathbb{I} for $\gamma = 1, 2, 3, 4$, respectively, corresponding to the four bonds incident on a vertex of the square lattice as shown in Fig. 1(a) and the sum is over all the γ bonds. Note that the $\gamma = 4$ (yellow) bond, which we refer to as the "identity" bond henceforth, has trivial orbital dependence. We consider $K_{1} = K_{2} = K$, unless specified otherwise. We identify two inequivalent intralayer flux plaquette operators $W_{\nu p} = \sigma^{z}_{\nu k} \sigma^{z}_{\nu n} \tau^{z}_{\nu i_{1}} \tau^{y}_{\nu j_{1}} \tau^{x}_{\nu n}$ and $W_{\nu p'} = \sigma^{z}_{\nu k} \sigma^{z}_{\nu n} \tau^{x}_{\nu n} \tau^{y}_{\nu l} \tau^{z}_{\nu m}$, each with \pm 1 eigenvalues. Both types of plaquette operators commute with the Hamiltonian and the Hilbert space is di-

vided into sectors of conserved fluxes. Note that the Ising form of the interlayer exchange is crucial to preserve $[W_{\nu p/p'}, H] =$ 0 [17]. The intralayer Hamiltonian can be solved by using a Majorana fermion representation of the Γ matrices [16], $H_K =$ $K \sum_{\langle ij\rangle_{\nu},\nu} i u_{\nu,ij}^{\gamma} [c_{\nu i}^{x} c_{\nu j}^{x} + c_{\nu i}^{y} c_{\nu j}^{y}]$ where $u_{\nu,ij}^{\gamma} = i b_{\nu i}^{\gamma} b_{\nu j}^{\gamma}$ (see the Supplemental Material (SM) for details [23]). This representation is redundant and the physical states in each layer must be restricted to the eigenstates of $D_{\nu j} = i b_{\nu j}^1 b_{\nu j}^2 b_{\nu j}^3 b_{\nu j}^4 c_{\nu j}^x c_{\nu j}^y$, with eigenvalues one. As in the Kitaev model, these constraints are imposed by the projection operator $P_{\nu} = \prod_{i} (1 + i)^{2}$ $D_{\nu i}$)/2. The intralayer bond operators $u_{\nu,ij}^{\gamma}$ commute with H_K and therefore are conserved with eigenvalues ± 1 . A \mathbb{Z}_2 gauge transformation at site i for layer ν involves flipping the signs of the Majorana fermions and bond operators, $c_{vi}^{\alpha} \rightarrow$ $-c_{\nu i}^{\alpha}$; $u_{\nu,\langle ij\rangle}^{\gamma} \rightarrow -u_{\nu,\langle ij\rangle}^{\gamma}$. We combine the Majorana fermions on the two layers to form complex fermions, $f_{\nu i} = (c_{\nu i}^{x} - c_{\nu i}^{x})^{2}$ ic_{vi}^{y})/2 such that $H_K = 2K \sum_{\langle ij \rangle} u_{v,ij}^{\gamma} [if_{vi}^{\dagger} f_{vj} + \text{H.c.}].$

According to Lieb's theorem [24], the GS manifold of H_K lies in the π -flux sector and consequently the eigenvalue of $W_{vp/p'} = \prod_{p/p'} u_{vij}^{\nu}$ is -1 in any GS configuration, for all square plaquettes. The spectrum is given by $E_K = \pm 4K\sqrt{\cos^2 k_x + \sin^2 k_y}$ which includes two inequivalent Dirac points at $(\pm \frac{\pi}{2}, 0)$.

Next, we represent the interlayer interaction in terms of the Majorana fermions: $H_J = -J \sum_i c_{1i}^x c_{1i}^y c_{2i}^x c_{2i}^y$. H_J commutes with the intralayer flux operators $W_{p/p'}$. However, the quartic form of the interlayer exchange precludes the exact solvability of H, which can be expressed as

$$H = 2K \sum_{\langle ij \rangle_{\gamma}, \nu} u_{\nu, ij}^{\gamma} [i f_{\nu i}^{\dagger} f_{\nu j} + \text{H.c.}]$$

$$+ 2J \sum_{i} [n_{1i} + n_{2i} - 1]^{2},$$
(2)

where $n_{\nu i} = f_{\nu i}^{\dagger} f_{\nu i}$.

Enhanced emergent symmetry. The Hamiltonian in Eq. (2) has a global U(1) symmetry in each layer $(\nu=1,2)$, $e^{-i\theta\sum_i\sigma_{\nu i}^z}He^{i\theta\sum_i\sigma_{\nu i}^z}=H$, a \mathbb{Z}_2 layer exchange symmetry \mathcal{X} , a particle-hole symmetry \mathcal{C} , and a time reversal symmetry \mathcal{T} . This results in a full symmetry group $G=O(2)_c\times O(2)_s\times\mathbb{Z}_2^{\mathcal{T}}$ of model (1), as detailed in the SM [23]. After the Majoranization, the two U(1) rotations manifest themselves as

$$U_c(\theta) f_{\nu i} U_c^{-1}(\theta) = e^{-i\theta} f_{\nu i},$$

$$U_s(\theta) f_{\nu i} U_s^{-1}(\theta) = e^{-i\kappa \theta} f_{\nu i},$$
(3)

where $\kappa=-1,1$ for $\nu=1,2$, respectively. This can be viewed as "charge:" $U_c=e^{i\theta\sum_{v^i}f_{v^i}^if_{v^i}}$, and "pseudospin:" $U_s=e^{i\theta\sum_{v^i}K_{v^i}^if_{v^i}}$ rotations, where $\kappa=+1(-1)$ for $\nu=1(2)$. The particle-hole symmetry $\mathcal C$ and U(1) charge rotations form the $O(2)_c$ subgroup, while the layer exchange $\mathcal X$ and U(1) pseudospin rotations form the $O(2)_s$ subgroup. Next, we fix the gauge by choosing $u_{\nu,ij}^{\gamma}=u_{ij}$, for both the layers and pick the π -flux configuration as discussed above. The resulting low-energy Hamiltonian (below the flux/vison gap) is a π -flux Hubbard model at half-filling with a hopping amplitude t=2K and interaction strength U=4J. It is well established [25] that the Hubbard model on a bipartite lattice possesses an enhanced $G'=SO(4)\times\mathbb{Z}_2^{\mathcal T}=\mathbb{Z}_2^{\mathcal T}\times SU(2)_c\times SU(2)_s/\mathbb{Z}_2$

TABLE I. Distinct ground state phases associated with different orientations of the Néel vector \mathbf{n} in (4). In each phase, the full symmetry $G = O(2)_c \times O(2)_s \times \mathbb{Z}_2^T$ of model (1) is spontaneously broken down to a different subgroup $H \leq G$, with an order parameter manifold $\mathcal{M} = G/H$. The gauge group for the associated topological order in each phase is also listed.

Néel vector	Unbroken subgroup H	G/H	Gauge group
$\mathbf{n} \parallel \hat{z}$	$O(2)_c \times U(1)_s \rtimes \mathbb{Z}_2^{\mathcal{X} \cdot \mathcal{T}}$	\mathbb{Z}_2	$\mathbb{Z}_2 \times \mathbb{Z}_2$
$\mathbf{n}\perp\hat{z}$	$O(2)_c \times \mathbb{Z}_2 \times \mathbb{Z}_2^{\tilde{\mathcal{T}}}$	S^1	\mathbb{Z}_2
$n_z \neq 0, n_x n_y \neq 0$	$O(2)_c imes \mathbb{Z}_2^{\mathcal{T}_{\mathbf{n}}}$	<i>O</i> (2)	\mathbb{Z}_2

symmetry. The equivalence established above shows that our model also exhibits an enhanced SO(4) symmetry at the low energy sector. In fact, this emergent SO(4) symmetry exists in any subspace with a fixed flux configuration. Emergent symmetries can play a key role to describe the low energy physics of strongly correlated systems including cuprates [26] and iron pnictides [27].

Quantum Monte Carlo studies have shown that the repulsive (J > 0) π -flux Hubbard model displays a phase transition from Dirac semimetal to an AFM Mott insulator at $J/K \sim 3$ $(U/t \sim 6)$ [18,19] [(see Fig. 1(c)]. Moreover, due to $J \rightarrow -J$ mapping in the Hubbard model, the phase diagram is symmetric for ferromagnetic (FM) and AFM interlayer exchange, for which the Néel order maps to superconducting and charge density wave orders.

The Néel vector of the AFM order

$$\mathbf{n} = \frac{1}{N} \sum_{i} \mathbf{n}_{i}, \quad \mathbf{n}_{i} = (-1)^{r_{ix} + r_{iy}} \langle f_{\mu i}^{\dagger} \boldsymbol{\sigma}_{\mu \nu} f_{\nu i} \rangle, \tag{4}$$

where N is the number of sites and $r_{ix(y)}$ is the x(y) coordinate of site i, can point along any direction on the Bloch sphere. Goldstone modes always arise since the emergent symmetry $G' = SO(4) \times \mathbb{Z}_2^T$ is spontaneously broken down to $H' = SU(2)_c \times U(1)_s \rtimes \mathbb{Z}_2^T$ in the Néel order (see the SM for details [23]). However, as we show below, different orientations of the Néel vector correspond to distinct ground states with different symmetry and topological properties, as summarized in Table I.

(i) The Néel vector points along the z direction, $\mathbf{n} \parallel \hat{z}$,

$$n_i^z = (-1)^{r_{ix} + r_{iy}} \langle f_{1i}^{\dagger} f_{1i} - f_{2i}^{\dagger} f_{2i} \rangle \neq 0.$$
 (5)

In terms of Majorana fermions, Eq. (5) takes the form $n_i^z = (-1)^{r_{ix}+r_{iy}}i(c_{1i}^xc_{1i}^y-c_{2i}^xc_{2i}^y)$. Note that n_i^z is invariant under local \mathbb{Z}_2 gauge transformations $(c_{vi}^x,c_{vi}^y) \to (-c_{vi}^x,-c_{vi}^y)$, hence corresponding to a physical operator $(-1)^{r_{ix}+r_{iy}}(\sigma_{1i}^z-\sigma_{2i}^z)$. In other words, n^z is a local order parameter of a Landau-type long range order.

The \mathbb{Z}_2 gauge fields for the two layers, $u_{1,ij}$ and $u_{2,ij}$, are decoupled, leading to a $\mathbb{Z}_2 \times \mathbb{Z}_2$ topological order described by four-component Abelian Chern-Simons theory [28] characterized by matrix $\mathbf{K} = \begin{pmatrix} 0 & 2 \\ 2 & 0 \end{pmatrix} \oplus \begin{pmatrix} 0 & 2 \\ 2 & 0 \end{pmatrix}$. However, the Goldstone mode of the Néel order

$$n^x + in^y \sim b_{\vec{k}=(\pi,\pi)} \sim \sum_i (-1)^{i_x + i_y} f_{2i}^{\dagger} f_{1i}$$
 (6)

is not a gauge-invariant quantity, but instead an anyon obeying mutual semion statistics with the vison in each layer. More precisely, the above Goldstone mode carries the gauge charge for the \mathbb{Z}_2 gauge field from each layer. One immediate consequence of the anyonic statistics of the Goldstone modes is that a single magnon cannot be created on top of the ground states for it vanishes under the onsite projection:

$$\left(\prod_{i,\nu} \frac{1 + D_{\nu,j}}{2}\right) b_{\vec{k} \approx (\pi,\pi)} |MF\rangle = 0, \tag{7}$$

where $|MF\rangle$ is the mean field ansatz (see the SM [23]). This is because the parity of fermions in each layer conserve separately in $|MF\rangle$, and the single "magnon" mode operator changes the fermion parity in each layer. Instead, the magnons have to be created in pairs

$$\left(\prod_{i,\nu} \frac{1 + D_{\nu,j}}{2}\right) b_{\vec{k}_1 \approx (\pi,\pi)} b_{\vec{k}_2 \approx (\pi,\pi)} |MF\rangle \neq 0 \tag{8}$$

due to the fact that any physical operator can only create a pair of anyons that are inverse of each other, but never a single anyon. Incorporating the gapless anyon b in (6) into the low energy description, the effective field theory for this algebraic spin liquid reads

$$\mathcal{L}_{ASL} = \sum_{I,J} \frac{\epsilon^{\mu\nu\rho}}{4\pi} a^{I}_{\mu} \mathbf{K}_{I,J} \partial_{\nu} a^{J}_{\rho} - \sum_{\alpha,I} \frac{\epsilon^{\mu\nu\rho}}{2\pi} A^{\alpha}_{\mu} \mathbf{q}^{\alpha}_{I} \partial_{\nu} a^{I}_{\rho}$$
$$+ \left| \left(-\mathrm{i}\partial_{\mu} - 2A^{s}_{\mu} - a^{1}_{\mu} - a^{2}_{\mu} + a^{3}_{\mu} - a^{4}_{\mu} \right)^{2} b \right|^{2} + \cdots,$$
(9)

where $A_{\mu}^{\alpha=c,s}$ label the charge and pseudospin external gauge fields, and

$$\mathbf{q}_c = (2, 0, 2, 0)^T, \quad \mathbf{q}_s = (2, 0, -2, 0)^T$$
 (10)

are the charge and pseudospin vectors [28] for the Chern-Simons theory.

(ii) The Néel vector lies inplane, e.g., $\mathbf{n} \perp \hat{z}$ with

$$n^{+} \equiv n_{i}^{x} + i n_{i}^{y} = (-1)^{r_{ix} + r_{iy}} \langle f_{1i}^{\dagger} f_{2i} \rangle \neq 0.$$
 (11)

Unlike n^z , the in-plane components, n^x and n^y , are not gauge invariant as the local gauge transformation maps $n^{x(y)} \rightarrow -n^{x(y)}$. However, a nonlocal gauge invariant correlator can be defined as [29]

$$C^{x(y)}(r,r') = \langle n^{x(y)}(r)B(r,r')n^{x(y)}(r')\rangle, \tag{12}$$

where the gauge string for fermions, $B(r, r') = \prod_{ij \in (r,r')} u_{1ij}u_{2ij}$, connects operators at the end sites (r, r'). The value of $C^{x(y)}(r, r')$ is the same in all gauge choices. Therefore, the ground state, symmetrized over all gauge configurations through the projection procedure, also has the same value of $C^{x(y)}(r, r')$, signifying a string order parameter. Physically, the long-range string order corresponds to the condensation of anyon b in the field theory (9), hence breaking the gauge group down to \mathbb{Z}_2 via the Higgs mechanism [30].

An alternative way to understand the gauge structure is to notice the following local order parameter for the in-plane Néel order

$$S_{\langle i,j\rangle}^{+} \equiv \langle n_i^{+} B(i,j) n_j^{+} \rangle \tag{13}$$

for a pair of nearest neighbor sites $\langle i,j \rangle$. Due to the mutual braiding phase of $e^{i\pi}$ between a vison and a fermion in each layer, a vison from layer 1 (or 2) is nothing but a vortex for the above local order parameter, since $S^+_{\langle i,j \rangle}$ acquires a $e^{\pm 2\pi i}$ phase as it travels around a vison from layer 1 (2). The logarithmic confinement of vortices in the in-plane Néel phase suggest that the vison from layer 1 (or 2) is confined, therefore reducing the $Z_2 \times Z_2$ gauge group down to Z_2 . A similar conclusion can be drawn if the Néel vector has both in-plane and \hat{z} components.

In general, the ground state can have both nonzero outof-plane (n^z) and in-plane (n^x, n^y) components. The term, "magnetic fragmentation" is coined for phases that display a coexistence of a local Landau-type order parameter and a nonlocal topological order [20,31–35]. Magnetic fragmentation is theoretically predicted [31] and experimentally observed [20] in spin ice materials such as $Nd_2Zr_2O_7$ where a local AFM order coexists with a spin liquid with FM correlations. We also point out that the Hubbard model mapping remains valid for any J value since the interlayer exchange term, H_J , commutes with the plaquette operators. Therefore, even with a large Jparameter, no fluxes are excited, preserving this mapping. The conclusions we draw from the Hubbard model rely on mean-field order parameters. Next, we underpin these results by a perturbative analysis.

Perturbative analysis in the limit of large interlayer exchange. We corroborate the results of the Hubbard model [Eq. (2)] by considering the bilayer in the large-J limit, without reference to the Majorana representation [Eq. (1)], on a torus. We introduce effective pseudospin and orbital DOF appropriate to this limit. We next derive effective models on the large-J GS manifold to fourth order in the intralayer coupling K. By analogy to the Hubbard model, we distinguish between cases with (i) \mathbb{Z}_2 and (ii) $\mathbb{Z}_2 \times \mathbb{Z}_2$ topological order. For (i), we show that the GS manifold is a state of uniform π flux with a finite $C^{x(y)}$ correlator [Eq. (12)]. We also demonstrate that the GS manifold has fourfold topological degeneracy and that the visons are confined. For (ii), we also obtain a GS with uniform π flux, which has sixteenfold topological degeneracy and deconfined vison excitations. These results naturally lead to the conclusion that the two phases are separated by a topological phase transition.

Effective degrees of freedom. We first introduce the effective pseudospin and orbital DOF. For K=0 and finite FM interlayer interactions (J<0), the spins on overlapping sites form GS doublets $|\uparrow_1\uparrow_2\rangle, |\downarrow_1\downarrow_2\rangle$. These can be represented by a bilayer pseudospin

$$\eta_i^z = \frac{1}{4} (\sigma_{1i}^z + \sigma_{2i}^z), \quad \eta_i^{\pm} = \frac{1}{4} \sigma_{1i}^{\pm} \sigma_{2i}^{\pm}, \tag{14}$$

obeying an SU(2) algebra. In addition, the orbital DOF for each pair of overlapping sites form a four-dimensional Hilbert space, corresponding to one singlet and three triplet configurations. To represent these states, we introduce the interlayer orbital operators $q_i^{\gamma} = \tau_{1i}^{\gamma} \tau_{2i}^{\gamma}$, $\gamma = x, y, z$, which mutually commute as $[q_i^{\alpha}, q_i^{\beta}] = 0$. The four orbital states can be labeled by the three eigenvalues $q_i^{\gamma} = \pm 1$, constrained to obey $\prod_{\gamma} q_i^{\gamma} = -1$. The Hilbert space thus includes all states of the form

$$|\{\eta^z\}, \{q^\gamma\}\rangle = |\{\eta_i^z\}\rangle \otimes |\{(q_i^x, q_i^y, q_i^z)\}\rangle, \tag{15}$$

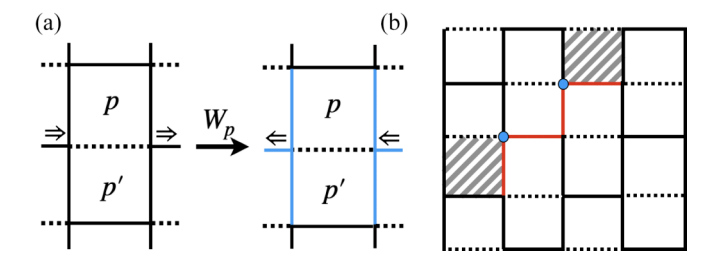


FIG. 2. Illustration of the pseudospin and bond $(\eta - \rho)$ configurations. (a) Effect of flux operator $W_{\nu p}$ on a state with fixed ρ_{ij}^{γ} bonds. $W_{\nu p}$ changes the signs of the bonds marked in blue. It also changes the signs of $\eta^{x/y}$ pseudospins on the identity (dashed) bond. (b) String defect, with red lines indicating bonds with signs opposite to the background bonds, marked in black. The string shown here is created by operating with $\tau_{\nu i}^{x}$ on any orbital state along the sites marked with blue dots. When operating on the GS in Eq. (20), the τ 's change the fluxes on the hashed plaquettes, since they ant-commute with $W_{\nu p/p'}$. Consequently, this open string terminates with a pair of visons.

with the implicit local constraint. Pairs of nearest-neighbor $q_{i/i}^{\gamma}$ define the bond variables

$$\rho_{ij}^{\gamma} = q_i^{\gamma} q_i^{\gamma} \tag{16}$$

which take on values of ± 1 for $\gamma \in \{x, y, z\}$, while they are trivially equal to one for additional identity bonds, labeled by $\rho^{\gamma=\mathrm{I}} \equiv 1$. To any $\{q_i^{\gamma}\}$ configuration, we can associate a unique $\{\rho_{ij}^{\gamma}\}$ bond configuration, while the converse is not true. Orbital states like $|\phi\rangle_0 = |\forall\,q_i^{\gamma} = -1\rangle$, which have uniform $\rho_{ij}^{\gamma} = 1$, play an important role in all subsequent discussions.

Defects in $|\phi\rangle_0$ take the form of strings of negative bonds as shown in Fig. 2(b). Defects in both pseudospin and ρ_{ij}^{γ} bonds are introduced by operating with the flux operators $W_{\nu p/p'}$. Each of these flips the pseudospin components along x/y as $\eta_{n,k}^{x/y} \to -\eta_{n,k}^{x/y}$ in the corresponding unit cell [Fig. 2(a)]. Each also changes the signs of all six ρ^{γ} bonds connected with sites n, k. Note that any string defect cannot be eliminated by application of $W_{\nu p/p'}$ operators.

Effective Hamiltonian. The effective Hamiltonian $H_{\eta-\rho}$, projected onto the K=0 GS manifold, reads

$$H_{\eta-\rho} = H_{g_2} + H_{g_4},\tag{17}$$

where

$$H_{g_2} = g_2 \left[\sum_{\langle ij \rangle} \eta_i^z \eta_j^z + \sum_{\langle ij \rangle_{\gamma}} \frac{1}{2} (\eta_i^+ \eta_j^- + \eta_i^- \eta_j^+) \rho_{ij}^{\gamma} \right] + \sum_i (-1)^{i_x + i_y} (h_x \eta_i^x + h_z \eta_i^z),$$
 (18)

is obtained at second order in K ($g_2 = K^2/4J$). Note the distinction between NN, in-plane pseudospins connected via variable and trivial identity ρ_{ij}^{γ} bonds, respectively. We introduce small perturbations $h_{x/z} > 0$ to explicitly break the continuous symmetry, enforcing the staggered pseudospin configurations along x/z, respectively. As it turns out, these respectively correspond to \mathbb{Z}_2 and $\mathbb{Z}_2 \times \mathbb{Z}_2$ topological order.

The fourth-order contribution is

$$H_{g_4} = g_4 \left[\sum_{\nu,p} \eta_p^{\square} W_{\nu p} + \sum_{\nu,p'} \eta_{p'}^{\square} W_{\nu p'} \right], \tag{19}$$

where $g_4 = K^4/J^3$. η_p^{\square} and $\eta_{p'}^{\square}$ include linear combinations of products of η and q^{γ} operators around p/p' plaquettes. H_{g_2} commutes with all flux operators for $h_x \to 0$, while this always holds for H_{g_4} . Technical details and derivations related to the effective Hamiltonian and the following sections are relegated to the SM [23].

 \mathbb{Z}_2 topological order. We consider $H_{\eta-\rho}$ with $h_x>0$ and $h_z=0$ on a torus. Exact diagonalization calculations indicate that the GS manifold of H_{g_2} includes $|\eta_{xx},\phi_0\rangle$, with η_{xx} denoting a finite staggered pseudospin along x (see the SM [23]). Importantly, any configuration with string defects in the ρ^{γ} bonds are gapped, with an energy cost which scales as the string length.

We next consider the evolution of the GS manifold at H_{g_4} level for $h_x \ll g_4 \ll g_2$. In the SM [23] we show that exact diagonalization calculations indicate H_{g_4} projects $|\eta_{xx}, \phi_0\rangle$ onto a state of uniform π flux per plaquette:

$$|\Psi_{\rm GS}\rangle = \prod_{\nu,p,p'} \frac{(1 - W_{\nu p})(1 - W_{\nu p'})}{4} |\tilde{\eta}_{xx};\phi_0\rangle + O\left(\frac{h_x}{g_4}\right).$$
 (20)

Note that $\tilde{\eta}_{xx}$ is a state of staggered pseudospins including corrections at both H_{g_2} and H_{g_4} levels. This is a state of definite π flux since $W_{vp}(1-W_{vp})=-(1-W_{vp})$. Moreover, all $W_{vp/p'}$ commute with the operator

$$\mathcal{D}_{ij}^{x} = \eta_i^{x} \left(\prod_{i'j' \in C_{ij}} \rho_{ij}^{\gamma} \right) \eta_j^{x}. \tag{21}$$

Consequently, the latter has a finite expectation value in $|\Psi_{\rm GS}\rangle$ for any pair of i,j, reflecting a locking of pseudo-spin and ρ_{ij}^{γ} bond configuration. Moreover, \mathcal{D}_{ij}^{x} is equivalent to a gauge-invariant correlator of the Hubbard model corresponding to an in-plane Néel vector [Eq. (12)]. The \mathbb{Z}_2 topological order corresponds to the second row in Table I.

Note that any state with an open string defect, obtained by first including strings in ϕ_0 , involves one or more visons on the plaquettes at each end [Fig. 2(b)]. As the energy of this excitation depends on the string length and diverges for infinite vison separation, it follows that the latter are confined in an infinite system.

 $\mathbb{Z}_2 \times \mathbb{Z}_2$ topological order. In this case, we consider $H_{\eta-\rho}$ with $h_z > 0$ and $h_x = 0$. By analogy with the case with \mathbb{Z}_2 topological order, the GS manifold of H_{g_2} now includes $|\eta_{zz}, \phi_0\rangle$, where η_{zz} indicates finite staggered pseudospins

along z. Similarly, any open string defects are gapped. However, in contrast to the case for \mathbb{Z}_2 topological order, the gap for these excitations remains finite for arbitrary string length, in the infinite-system size. In the same limit, states with strings forming noncontractible loops become degenerate with $|\phi_0\rangle$ for $h_z\gg g_{2/4}$.

The effect of H_{g_4} is analogous to the case with \mathbb{Z}_2 topological order. Consequently, the GS has the form in Eq. (20), with the replacement $|\tilde{\eta}_{xx};\phi_0\rangle \rightarrow |\tilde{\eta}_{zz};\phi_0\rangle$, indicating a surviving pseudospin staggering. While the two-point correlator for the η^z pseudospins is always finite, \mathcal{D}_{ij}^x vanishes for infinite separation as in the Hubbard model with $\mathbb{Z}_2 \times \mathbb{Z}_2$ topological order.

Since the energy cost of an open string remains finite even in an infinite-size system, the visons are deconfined. Similarly, as states with noncontractible loops of negative ρ^{γ} bonds become degenerate with the GS, in the limit of infinite systemsize, the latter acquires additional topological degeneracy. Consequently, this entails a sixteenfold topological degeneracy on the torus, consistent with $\mathbb{Z}_2 \times \mathbb{Z}_2$ topological order corresponding to row 1 in Table I.

Conclusion and outlook. We have studied a bilayer adaptation of a QSL model on a square lattice with Kitaev-type interactions. We have shown that the low energy model exhibits an AFM Mott transition which corresponds to magnetic fragmentation in terms of the original DOF. We have corroborated these results by a perturbative calculation for the topological degeneracy, which is consistent with field theory analysis. The analysis we have presented here may be of particular value as a largely tractable yet highly nontrivial instance of magnetic fragmentation.

Interesting future directions include examining the role of fluctuations on the emergent symmetry which may reduce the ground state manifold via order by disorder [36–38]. Another direction is to generalize our mechanism for fractionalized Goldstone modes in bilayer systems to multilayer systems with larger emergent symmetries, such as SU(N).

The study of moiré superlattices of QSLs is another intriguing direction [29,39]. Our work suggests that manifold new phenomena arising from a combination of emergent symmetry and strong interactions are awaiting discovery here, providing a new vista on strongly correlated magnetism.

Acknowledgments. We thank Nandini Trivedi and Natalia Perkins for fruitful discussions. O.E. acknowledges support from the NSF Award No. DMR-2234352. Y.M.L. is supported by the NSF under Award No. DMR-2011876. E.M.N. acknowledges support by the NSF under Grant No. DMR-2220603. This work in part supported by the Deutsche Forschungsgemeinschaft (DFG) via SFB 1143 (project-id 247310070) and cluster of excellence ct.qmat (EXC 2147, project-id 390858490).

^[1] C. Broholm, R. J. Cava, S. A. Kivelson, D. G. Nocera, M. R. Norman, and T. Senthil, Quantum spin liquids, Science **367**, eaay0668 (2020).

^[2] L. Balents, Spin liquids in frustrated magnets, Nature (London) 464, 199 (2010).

^[3] L. Savary and L. Balents, Quantum spin liquids: A review, Rep. Prog. Phys. 80, 016502 (2017).

^[4] R. Moessner and J. E. Moore, *Topological Phases of Matter* (Cambridge University Press, Cambridge, UK, 2021).

- [5] Y. Zhou, K. Kanoda, and T.-K. Ng, Quantum spin liquid states, Rev. Mod. Phys. 89, 025003 (2017).
- [6] J. Knolle and R. Moessner, A field guide to spin liquids, Annu. Rev. Condens. Matter Phys. 10, 451 (2019).
- [7] X.-G. Wen, Colloquium: Zoo of quantum-topological phases of matter, Rev. Mod. Phys. 89, 041004 (2017).
- [8] A. Kitaev, Anyons in an exactly solved model and beyond, Ann. Phys. 321, 2 (2006).
- [9] S. Hwan Chun, J.-W. Kim, J. Kim, H. Zheng, C. C. Stoumpos, C. D. Malliakas, J. F. Mitchell, K. Mehlawat, Y. Singh, Y. Choi, T. Gog, A. Al-Zein, M. M. Sala, M. Krisch, J. Chaloupka, G. Jackeli, G. Khaliullin, and B. J. Kim, Direct evidence for dominant bond-directional interactions in a honeycomb lattice iridate Na₂IrO₃, Nat. Phys. 11, 462 (2015).
- [10] K. Kitagawa, T. Takayama, Y. Matsumoto, A. Kato, R. Takano, Y. Kishimoto, S. Bette, R. Dinnebier, G. Jackeli, and H. Takagi, A spin-orbital-entangled quantum liquid on a honeycomb lattice, Nature (London) 554, 341 (2018).
- [11] H. Takagi, T. Takayama, G. Jackeli, G. Khaliullin, and S. E. Nagler, Concept and realization of Kitaev quantum spin liquids, Nat. Rev. Phys. 1, 264 (2019).
- [12] I. Lee, F. G. Utermohlen, D. Weber, K. Hwang, C. Zhang, J. van Tol, J. E. Goldberger, N. Trivedi, and P. C. Hammel, Fundamental Spin Interactions Underlying the Magnetic Anisotropy in the Kitaev Ferromagnet CrI₃, Phys. Rev. Lett. 124, 017201 (2020).
- [13] Y. Cao, V. Fatemi, S. Fang, K. Watanabe, T. Taniguchi, E. Kaxiras, and P. Jarillo-Herrero, Unconventional superconductivity in magic-angle graphene superlattices, Nature (London) 556, 43 (2018).
- [14] T. Devakul, V. Crépel, Y. Zhang, and L. Fu, Magic in twisted transition metal dichalcogenide bilayers, Nat. Commun. 12, 6730 (2021).
- [15] S. Y. F. Zhao, N. Poccia, X. Cui, P. A. Volkov, H. Yoo, R. Engelke, Y. Ronen, R. Zhong, G. Gu, S. Plugge, T. Tummuru, M. Franz, J. H. Pixley, and P. Kim, Emergent interfacial superconductivity between twisted cuprate superconductors, arXiv:2108.13455.
- [16] R. Nakai, S. Ryu, and A. Furusaki, Time-reversal symmetric Kitaev model and topological superconductor in two dimensions, Phys. Rev. B 85, 155119 (2012).
- [17] U. F. P. Seifert, X.-Y. Dong, S. Chulliparambil, M. Vojta, H.-H. Tu, and L. Janssen, Fractionalized Fermionic Quantum Criticality in Spin-Orbital Mott Insulators, Phys. Rev. Lett. 125, 257202 (2020).
- [18] Y. Otsuka, S. Yunoki, and S. Sorella, Mott transition in the 2d Hubbard model with π -flux, JPS Conf. Proc. 3, 013021 (2014).
- [19] Y. Otsuka, S. Yunoki, and S. Sorella, Universal Quantum Criticality in the Metal-Insulator Transition of Two-Dimensional Interacting Dirac Electrons, Phys. Rev. X 6, 011029 (2016).
- [20] S. Petit, E. Lhotel, B. Canals, M. Ciomaga Hatnean, J. Ollivier, H. Mutka, E. Ressouche, A. R. Wildes, M. R. Lees, and G. Balakrishnan, Observation of magnetic fragmentation in spin ice, Nat. Phys. 12, 746 (2016).
- [21] C. Wu, D. Arovas, and H.-H. Hung, Γ-matrix generalization of the Kitaev model, Phys. Rev. B **79**, 134427 (2009).
- [22] H. Yao, S.-C. Zhang, and S. A. Kivelson, Algebraic Spin Liquid in an Exactly Solvable Spin Model, Phys. Rev. Lett. **102**, 217202 (2009).

- [23] See Supplemental Material at http://link.aps.org/supplemental/ 10.1103/PhysRevResearch.5.L022062 for details.
- [24] E. H. Lieb, Flux Phase of the Half-Filled Band, Phys. Rev. Lett. 73, 2158 (1994).
- [25] C. N. Yang and S.C. Zhang, SO(4) symmetry in a Hubbard model, Mod. Phys. Lett. B 04, 759 (1990).
- [26] E. Demler, W. Hanke, and S.-C. Zhang, SO(5) theory of antiferromagnetism and superconductivity, Rev. Mod. Phys. 76, 909 (2004).
- [27] D. Podolsky, H.-Y. Kee, and Y. B. Kim, Collective modes and emergent symmetry of superconductivity and magnetism in the iron pnictides, Europhys. Lett. **88**, 17004 (2009).
- [28] X. G. Wen and A. Zee, Classification of abelian quantum hall states and matrix formulation of topological fluids, Phys. Rev. B 46, 2290 (1992).
- [29] E. M. Nica, M. Akram, A. Vijayvargia, R. Moessner, and O. Erten, Kitaev spin-orbital bilayers and their moiré superlattices, npj Quantum Mater. **8**, 9 (2023).
- [30] T. H. Hansson, V. Oganesyan, and S. L. Sondhi, Superconductors are topologically ordered, Ann. Phys. 313, 497 (2004).
- [31] M. E. Brooks-Bartlett, S. T. Banks, L. D. C. Jaubert, A. Harman-Clarke, and P. C. W. Holdsworth, Magnetic-Moment Fragmentation and Monopole Crystallization, Phys. Rev. X 4, 011007 (2014).
- [32] E. Lefrançois, V. Cathelin, E. Lhotel, J. Robert, P. Lejay, C. V. Colin, B. Canals, F. Damay, J. Ollivier, B. Fåk, L. C. Chapon, R. Ballou, and V. Simonet, Fragmentation in spin ice from magnetic charge injection, Nat. Commun. 8, 209 (2017).
- [33] A. Zorko, M. Pregelj, M. Klanjšek, M. Gomilšek, Z. Jagličić, J. S. Lord, J. A. T. Verezhak, T. Shang, W. Sun, and J.-X. Mi, Coexistence of magnetic order and persistent spin dynamics in a quantum kagome antiferromagnet with no intersite mixing, Phys. Rev. B 99, 214441 (2019).
- [34] C. Mauws, A. M. Hallas, G. Sala, A. A. Aczel, P. M. Sarte, J. Gaudet, D. Ziat, J. A. Quilliam, J. A. Lussier, M. Bieringer, H. D. Zhou, A. Wildes, M. B. Stone, D. Abernathy, G. M. Luke, B. D. Gaulin, and C. R. Wiebe, Dipolar-octupolar ising antiferromagnetism in Sm₂Ti₂O₇: A moment fragmentation candidate, Phys. Rev. B 98, 100401(R) (2018).
- [35] Y.-Q. Wang, C. Liu, and Y.-M. Lu, Theory of topological defects and textures in two-dimensional quantum orders with spontaneous symmetry breaking, arXiv:2211.13207.
- [36] E. F. Shender, Antiferromagnetic garnets with fluctuationally interacting sublattices, Zh. Eksp. Teor. Fiz. **83**, 326 (1982) [Sov. J. Exp. Theor. Phys. **56**, 178 (1982)].
- [37] C. L. Henley, Ordering Due to Disorder in a Frustrated Vector Antiferromagnet, Phys. Rev. Lett. 62, 2056 (1989).
- [38] A. G. Green, G. Conduit, and F. Krüger, Quantum order-bydisorder in strongly correlated metals, Annu. Rev. Condens. Matter Phys. 9, 59 (2018).
- [39] Z.-X. Luo, U. F. P. Seifert, and L. Balents, Twisted bilayer U(1) Dirac spin liquids, Phys. Rev. B 106, 144437 (2022).

Correction: Typographical errors in the NSF award numbers in the Acknowledgment section have been fixed.